ORIGINAL RESEARCH

Vadose Zone Journal

Chemical Modeling of Arsenic(III, V) and Selenium(IV, VI) Adsorption by Soils Surrounding Ash Disposal Facilities

Sabine Goldberg,* Seunghun Hyun, and Linda S. Lee

Leachate derived from coal ash disposal facilities is a potential anthropogenic source of As and Se to the environment. To establish a practical framework for predicting attenuation and transport of As and Se in ash leachates, the adsorption of As(III), As(V), Se(IV), and Se(VI) had been characterized in prior studies for 18 soils obtained downgradient from ash landfill sites and representing a wide range of soil properties. The constant capacitance model was applied for the first time to describe As(III), As(V), Se(IV), and Se(VI) adsorption on soils as a function of equilibrium solution As(III), As(V), Se(IV), and Se(VI) concentrations. Prior applications of the model had been restricted to describing Se(IV) and As(V) adsorption by soils as a function of solution pH. The constant capacitance model was applied for the first time to describe As(III) and Se(VI) adsorption by soils. The model was able to describe adsorption of these ions on all soils as a function of solution ion concentration by optimizing only one adjustable parameter, the anion surface complexation constant. This chemical model represents an advancement over adsorption isotherm equation approaches that contain two empirical adjustable parameters. Incorporation of these anion surface complexation constants obtained with the constant capacitance model into chemical speciation transport models will allow simulation of soil solution anion concentrations under diverse environmental and agricultural conditions.

ABBREVIATIONS: DCB, dithionite–citrate–bicarbonate.

ARSENIC and Se are trace elements toxic to animals, including humans, wildlife, and aquatic species. However, selenium is also a nutritionally essential trace element, with a very narrow range between deficiency and toxicity. Significant sources of As and Se to the environment are coal ash and fly ash. Currently in the United States, an estimated 67% of the boiler fly ash produced from coal-fired power plants is disposed of in landfills (Hall and Livingston, 2002). Therefore, dissolved As and Se in the leachate may enter adjacent water bodies and groundwater.

The major inorganic species found in soil solution are arsenite, As(III), and arsenate, As(V), for As and selenite, Se(IV), and selenate, Se(VI) for Se (Adriano, 1986). For each element, the toxic mode of action (Agency for Toxic Substances and Disease Registry, 2000, 2003), as well as the mobility, is dependent on the oxidation state. In most cases, greater toxicity has been observed for the more reduced species. Thus, As(III) is considerably more toxic than As(V) (Flower, 1977) and Se(IV) is considered more toxic than Se(VI) (Cobo Fernandez et al., 1993).

The valence states of As and Se in fly ash leachate are difficult to predict because of ash heterogeneity, slow dissolution and desorption kinetics, and microbial transformation processes (Eary et al., 1990). Fly ash leachates are either mixtures of As redox states or dominant in As(III) (Turner, 1981) or As(V) (Jackson and Miller, 1998). Comparable behavior is found for Se, with various fly ashes ranging from 5 to 100% Se(IV) (Jackson and Miller, 1998). For both As and Se, the oxidation–reduction rates are slow so that both redox states can coexist in soil solution (Masscheleyn et al., 1990, 1991).

Adsorption reactions by soil can attenuate As and Se concentrations in leachates from coal ash disposal facilities. Adsorption behavior is dependent on the redox state of the element, the soil pH, and the soil mineral type. Arsenic and Se adsorption are highly pH dependent. Arsenite is often considered to be more weakly bound than As(V). However, since the adsorption maxima for As(V) are around pH 4 to 6 (Goldberg et al., 2005), while As(III) adsorption peaks in the pH range 7 to 9 (Raven et al., 1998), As(III) often adsorbs to a greater extent than As(V) at high pH (Raven et al., 1998). Selenite is consistently more strongly adsorbed than Se(VI). While Se(VI) adsorbs on reference minerals such as Fe oxides (Balistrieri and Chao, 1990) and clays (Bar-Yosef and Meek, 1987), it adsorbs weakly or not at all on soils and is readily leached (Neal and Sposito, 1989).

Arsenite adsorbs via an inner-sphere adsorption mechanism, forming bidentate surface complexes on goethite (Manning

S. Goldberg, USDA-ARS, U.S. Salinity Laboratory, 450 W. Big Springs Rd., Riverside, CA 92507; S. Hyun, Div. of Environmental Science and Ecological Engineering, Korea Univ., Seoul 136-701, Korea; L.S. Lee, Dep. of Agronomy, Purdue Univ., West Lafayette, IN 47907. Received 22 Jan. 2008.
*Corresponding author (Sabine.Goldberg@ars.usda.gov).

Vadose Zone J. 7:1231–1238
doi:10.2136/vzj2008.0013

et al., 1998), ferrihydrite, hematite, and lepidocrocite (Ona-Nguema et al., 2005). In addition to bidentate complexes, minor amounts of monodentate As(III) surface complexes were found on goethite and lepidocrocite (Ona-Nguema et al., 2005). Results from Fourier-transform infrared spectroscopy (FTIR) combined with electrophoretic mobility and potentiometric titration data indicated monodentate attachment of As(III) on amorphous Fe and Al oxides (Suarez et al., 1998). Arsenate adsorbs via an inner-sphere adsorption mechanism, forming bidentate surface complexes on goethite, ferrihydrite (Waychunas et al., 1993), gibbsite (Ladeira et al., 2001), Mn oxide (Foster et al., 2003), and hematite (Catalano et al., 2007). Monodentate As(V) surface complexes were also observed on goethite and ferrihydrite (Waychunas et al., 1993). Results from FTIR spectroscopy combined with electrophoretic mobility and potentiometric titration data indicated monodentate attachment of As(V) on amorphous Fe oxide (Suarez et al., 1998). Selenite was found to adsorb as an inner-sphere bidentate surface complex on hematite (Catalano et al., 2006) and amorphous Al oxide (Peak, 2006). A mixture of monodentate and bidentate Se(IV) complexes was found on Mn oxide (Foster et al., 2003). Selenate adsorbs via an inner-sphere adsorption mechanism, forming bidentate surface complexes on goethite and amorphous Fe oxide (Suarez et al., 1998) and monodentate surface complexes on the Al oxide corundum (Peak, 2006).

Arsenic and Se adsorption on soils has been described using various modeling approaches. Such models include the empirical linear distribution coefficient, K_d (de Brouwere et al., 2004; Wang and Liu, 2005), the Freundlich adsorption isotherm equation (Elkhatib et al., 1984; Del Debbio, 1991; Smith et al., 1999; Burns et al., 2006; Hyun et al., 2006), and the Langmuir adsorption isotherm equation (Elsokkary, 1980; Singh et al., 1981; Jiang et al., 2005).

The distribution coefficient is defined as a linear function and therefore it usually describes adsorption data only across a very restricted solution concentration range. This behavior was observed by Wang and Liu (2005) for Se(IV) adsorption by a calcareous soil. For ions whose adsorption behavior is pH dependent, K_d is not constant. Variations in K_d with solution pH were found for As(V) adsorption by soils (de Brouwere et al., 2004). The Freundlich adsorption isotherm is strictly valid only for ion adsorption at low aqueous concentrations (Sposito, 1984), but has often been used to describe adsorption across the entire concentration range investigated. Application of various isotherm equations often leads to fits of comparable quality (Singh and Pant, 2004). When model fit appears poor, a two-site Langmuir adsorption isotherm equation is often formulated for simultaneous adsorption onto two types of surface sites. Not surprisingly, due to the increase in the number of adjustable parameters, the fit to adsorption data with the two-site Langmuir isotherm is often much improved over the single-site Langmuir isotherm. This was the case for Se(IV) and Se(VI) adsorption (Singh et al., 1981) and As(V) adsorption (Jiang et al., 2005) by soils. Although isotherm equations are often excellent at describing ion adsorption, they are simply empirical numerical relationships used to fit adsorption data and their parameters are only valid for the conditions under which the experiment was conducted. Adherence of experimental data to an adsorption isotherm equation alone provides no information about the chemical reaction mechanism (Sposito, 1982). Independent experimental evidence for an adsorption process must be available before any chemical significance can be assigned to isotherm equation parameters. Unfortunately, this caveat has been almost universally ignored in adsorption studies.

Surface complexation models, unlike empirical adsorption isotherm equations, are chemical models that define surface species, chemical reactions, mass balances, and charge balance and contain molecular features that can be given thermodynamic significance (Sposito, 1983). With these models, thermodynamic properties such as solid-phase activity coefficients and equilibrium constants are calculated mathematically. The major advancement of the surface complexation models is consideration of charge on both the adsorbate ion and the adsorbent surface. These models can also provide insight into the stoichiometry and reactivity of adsorbed species. Surface complexation models have the potential to be predictive in nature and applicable to more than one field site.

Applications of surface complexation models to describe As and Se adsorption by soils have been more limited and restricted to the constant capacitance model (Goldberg and Glaubig, 1988a,b; Sposito et al., 1988; Goldberg et al., 2005, 2007), the diffuse layer model (Lumsdon et al., 2001), and the CD-MUSIC model (Gustafsson, 2001, 2006). In most surface complexation modeling, adsorption isotherm data are described by assuming that the ion adsorbs to one or at most two average sets of reactive surface sites. This is clearly a gross simplification since natural materials are complex multisite mixtures having a variety of surface functional groups.

Two types of approaches exist for modeling adsorption on complex mineral assemblages such as soils (Davis et al., 1998). Component additivity attempts to predict adsorption on soils using the results of a surface characterization of the soil along with experimental data and model parameters obtained for adsorption by pure reference minerals. In the generalized composite approach, it is assumed that the adsorption behavior of a soil can be described by surface complexation reactions written for generic surface functional groups that represent average properties of the soil as a whole rather than of specific mineral phases.

Component additivity approaches have been used to describe As(V) adsorption by soil with the diffuse layer model (Lumsdon et al., 2001) and the CD-MUSIC model (Gustafsson, 2001). Lumsdon et al. (2001) described As(V) adsorption in a contaminated soil profile by assuming that the principal reactive adsorbent was amorphous Fe oxide. The modeling was only successful in describing adsorption in the two layers containing the most extractable Fe. The description of adsorption in three other horizons was either greatly over- or underestimated. Gustafsson (2001) used the CD-MUSIC model to describe As(V) adsorption on a spodic B horizon. He assumed that the reactive components were allophane and amorphous Fe oxide and used As(V) surface complexation constants obtained on gibbsite to represent allophane. The fit of the CD-MUSIC model was generally very good, although not quantitative across the entire range of As(V) surface coverages. The use of component additivity approaches is severely restricted by the fact that most soils have mixed mineralogy.

Chemical significance is optimized if as many surface complexation model parameters as possible are obtained experimentally. If there is no independent experimental evidence allowing the determination of the exact structure of adsorbed surface com-

plexes, the use of models having chemical simplicity and a small number of adjustable parameters is preferable.

Generalized composite approaches have been used successfully in the application of the constant capacitance model to describe Se(IV) (Goldberg and Glaubig, 1988a; Sposito et al., 1988; Goldberg et al., 2007) and As(V) adsorption by soils (Goldberg and Glaubig, 1988b; Goldberg et al., 2005). The constant capacitance model has not yet been applied to describe As(III) or Se(VI) adsorption by soils. Prior studies of Se(IV) (Goldberg and Glaubig, 1988a; Sposito et al., 1988; Goldberg et al., 2007) and As(V) adsorption (Goldberg and Glaubig, 1988b; Goldberg et al., 2005) by soils have been restricted to the description of adsorption as a function of solution pH. The model has not yet been used to describe As or Se adsorption data as a function of equilibrium solution As or Se concentration.

Therefore, for the present study, the constant capacitance model was chosen, both because of its long successful history of describing adsorption by soils and for its chemical simplicity. Our objective was to apply the constant capacitance model to describe As(III), As(V), Se(IV), and Se(VI) adsorption as a function of equilibrium solution As(III), As(V), Se(IV), and Se(VI) concentrations by a set of soils obtained downgradient of three different fly ash disposal facilities. The adsorption isotherms of these soils had been previously described using the Freundlich adsorption isotherm equation for Se(VI) and Se(IV) (Hyun et al., 2006) and As(V) and As(III) (Burns et al., 2006). This will be the first application of the constant capacitance model to describe As(III) and Se(VI) adsorption by soils.

Materials and Methods

A total of 18 soil samples were collected from three utility sites within the United States (identified as Northeast [NE], Southeast [SE], and Midwest [MW]) where ash landfills are presently in use or are planned. For each site, soils were sampled downgradient from the landfill areas at depths ranging from 3 to 18.3 m. Previously determined soil properties (Burns et al., 2006; Hyun et al., 2006) along with surface areas are summarized in Table 1. Ranges of these properties were: pH, 4.4 to 7.3; clay, 1 to 29%; sand, 9 to 97%; organic matter, 0.2 to 1.5%; cation exchange capacity, 1.4 to 15.5 $cmol_c\ kg^{-1}$; dithionite–citrate–bicarbonate (DCB) extractable Fe, 5.9 to 32 $g\ kg^{-1}$; DCB-extractable Al, 0.17 to 1.3 $g\ kg^{-1}$; oxalate-extractable Fe, 0.15 to 5.5 $g\ kg^{-1}$; oxalate-extractable Al, 0.10 to 0.53 $g\ kg^{-1}$; and 15-s DCB-extractable Fe, 0.01 to 1.62 $g\ kg^{-1}$. The clay mineralogy of the NE and SE soils is dominated by illite and kaolinite. Mineral identification of the clay fraction for the MW soils was not possible because they contained <1% clay. Soil surface areas for 15 of the 18 soils were determined using ethylene glycol monoethyl ether adsorption as described by Cihacek and Bremner (1979). At the time when surface areas were determined, three of the 18 soil samples had been depleted.

Arsenic and Se adsorption isotherms were measured for all 18 soils from 1 mmol L^{-1} $CaSO_4$ solution using a batch technique. Initial anion concentrations ranged from 0 to 66 μmol L^{-1} for As(V), 0 to 16 μmol L^{-1} for As(III), 0 to 34 μmol L^{-1} for Se(IV), and 0 to 13 μmol L^{-1} for Se(VI). Solid suspension density was 20 g L^{-1} for As(V), 50 g L^{-1} for As(III) and Se(IV), and 100 g L^{-1} for Se(VI). Equilibration times were 16 h for As(III) and Se(IV) and 48 h for As(V) and Se(VI). No release of As or Se was observed on the zero-anion-added treatments. Suspensions containing the reduced species were equilibrated for a shorter time due to concerns that a significant amount of oxidation would occur. Preliminary analyses showed that oxidation of As was insignificant (Burns et al., 2006) and oxidation of Se was <10% during the 16-h period (Hyun et al., 2006). It is still possible that trace amounts of As(V) could be found in the As(III) solutions. Additional experimental details for the adsorption isotherm determinations and Freundlich adsorption isotherm model fits have been provided in Burns et al. (2006) and Hyun et al. (2006).

The constant capacitance model (Stumm et al., 1980) was used to describe As and Se adsorption isotherms on the soils. The computer program FITEQL 3.2 (Herbelin and Westall, 1996) was used to fit As and Se surface complexation constants to the experimental adsorption data. In the model, the protonation and dissociation reactions for the surface functional group, *S*OH (where *S*OH represents a reactive surface hydroxyl bound to a metal ion, *S* [Al, Fe, or Mn] in the oxide mineral or an aluminol group on the clay particle edge) are defined as

$$SOH_{(s)} + H^+_{(aq)} \leftrightarrow SOH^+_{2(s)} \quad [1]$$

$$SOH_{(s)} \leftrightarrow SO^-_{(s)} + H^+_{(aq)} \quad [2]$$

TABLE 1. Selected physical and chemical properties of soils used in this study.

Soil	Sand	Clay	OM†	S_A‡	CEC	DCB-Fe§	DCB-Al§	Ox-Fe¶	Ox-Al¶	DCB-Fe15s#
	%			$m^2\ g^{-1}$	$cmol\ kg^{-1}$	$g\ kg^{-1}$				
NE1 25–30	33	17	0.5	21.8	15.5	5.92	0.27	0.32	0.24	0.27
NE1 35–40	40	25	0.5	27.1	12.6	6.03	0.61	5.47	0.53	0.65
NE2 10–15	60	17	1	19.6	4.7	31.8	1.20	1.58	0.51	0.99
NE2 16–21	59	13	0.5	12.4	2.45	11.4	0.63	1.09	0.36	0.53
NE3 50–54	9	29	0.6	50.0	13.2	22.5	1.07	1.75	0.48	1.62
NE4 46–50	57	15	0.9	18.2	5.8	18.3	1.30	1.59	0.50	1.04
SE1 48.5	62	5	0.6	16.5	4.3	7.10	0.45	0.58	0.49	0.15
SE1 60	56	5	0.7	32.6	4.8	14.9	0.90	0.76	0.42	0.33
SE2 23.5	66	3	0.3	13.6	4.1	8.40	0.18	0.41	0.31	0.06
SE3 5.5	66	5	0.4	7.2	3.1	6.21	0.28	0.23	0.40	0.08
SE3 38.5	62	3	0.4	2.1	4.1	6.65	0.15	0.50	0.24	0.07
MW1 17	93	3	0.3	3.0	3	4.54	0.61	0.57	0.46	0.07
MW2 17	95	1	0.4	4.3	1.4	3.31	0.38	0.26	0.25	0.03
MW2 25	97	1	0.4	0.7	1.4	3.14	0.18	0.22	0.10	0.01
MW3 17	95	1	0.2	2.7	1.7	2.72	0.39	0.30	0.38	0.02
MW3 23	95	1	0.5	21.8	1.4	2.96	0.17	0.24	0.11	0.01

† Soil organic matter.

‡ Surface area determined using ethylene glycol monoethyl ether adsorption as described by Cihacek and Bremner (1979).

§ Dithionite–citrate–bicarbonate extractable Fe and Al.

¶ Oxalate (pH 3) extractable Fe and Al.

Quickly (15-s) dissolved Fe in DCB solution.

In the constant capacitance model, all surface complexation reactions form inner sphere surface complexes. The surface complexation reactions for As adsorption are defined as

$$SOH_{(s)} + H_3AsO_{4(aq)} \leftrightarrow SHAsO^-_{4(s)} + H^+_{(aq)} + H_2O \quad [3]$$

$$SOH_{(s)} + H_3AsO_{3(aq)} \leftrightarrow SH_2AsO_{3(s)} + H_2O \quad [4]$$

and for Se adsorption as

$$SOH_{(s)} + H_2SeO_{4(aq)} \leftrightarrow SSeO^-_{4(s)} + H^+_{(aq)} + H_2O \quad [5]$$

$$SOH_{(s)} + H_2SeO_{3(aq)} \leftrightarrow SSeO^-_{3(s)} + H^+_{(aq)} + H_2O \quad [6]$$

By convention, surface complexation reactions in the constant capacitance model are written starting with completely undissociated acid species; however, the model applications contain the aqueous speciation reactions for As and Se. The surface configurations were chosen because they correspond to the dominant As and Se solution species in the pH ranges investigated. Other possible surface species—SH_2AsO_4, $SAsO_4^{2-}$, $SHAsO_3^-$, $SHSeO_4$, and $SHSeO_3$—were considered and found to be insignificant during model optimization. Prior investigations of As(V) (Goldberg et al., 2005) and Se(IV) (Goldberg et al., 2007) adsorption by soils found that model fits where superior in quality (as measured by the goodness-of-fit criterion, V_Y, Eq. [22] below) when monodentate surface species rather than bidentate species were used. An additional complication when using bidentate surface species is that the surface complexation constants become dependent on the concentration of [*S*OH] because the [*S*OH] term is squared.

The intrinsic equilibrium constants for the protonation and dissociation reactions are

$$K_+(\text{int}) = \frac{[SOH_2^+]}{[SOH][H^+]}\exp\left(F\psi/RT\right) \quad [7]$$

$$K_-(\text{int}) = \frac{[SO^-][H^+]}{[SOH]}\exp\left(-F\psi/RT\right) \quad [8]$$

where F is the Faraday constant (C mol_c^{-1}), ψ is the surface potential (V), R is the molar gas constant (J mol^{-1} K^{-1}), T is the absolute temperature (K), and square brackets indicate concentrations (mol L^{-1}). The intrinsic equilibrium constants for As are

$$K^2_{As(V)}(\text{int}) = \frac{[SHAsO_4^-][H^+]}{[SOH][H_3AsO_4]}\exp\left(-F\psi/RT\right) \quad [9]$$

$$K^1_{As(III)}(\text{int}) = \frac{[SHAsO_3]}{[SOH][H_2AsO_3]} \quad [10]$$

and the Se intrinsic equilibrium constants are

$$K^2_{Se(VI)}(\text{int}) = \frac{[SSeO_4^-][H^+]}{[SOH][H_2SeO_4]}\exp\left(-F\psi/RT\right) \quad [11]$$

$$K^2_{Se(IV)}(\text{int}) = \frac{[SSeO_3^-][H^+]}{[SOH][H_2SeO_3]}\exp\left(-F\psi/RT\right) \quad [12]$$

The mass balance expressions for the surface functional group for As adsorption are

$$[SOH]_T = [SOH] + [SOH_2^+] + [SO^-] + [SHAsO_4^-] \quad [13]$$

$$[SOH]_T = [SOH] + [SOH_2^+] + [SO^-] + [SHAsO_3] \quad [14]$$

and for Se adsorption are

$$[SOH]_T = [SOH] + [SOH_2^+] + [SO^-] + [SSeO_4^-] \quad [15]$$

$$[SOH]_T = [SOH] + [SOH_2^+] + [SO^-] + [SSeO_3^-] \quad [16]$$

The charge balance expressions are

$$\text{for As(V): } \sigma = [SOH_2^+] - [SO^-] - [SHAsO_4^-] \quad [17]$$

$$\text{for As(III): } \sigma = [SOH_2^+] - [SO^-] \quad [18]$$

$$\text{for Se(VI): } \sigma = [SOH_2^+] - [SO^-] - [SSeO_4^-] \quad [19]$$

$$\text{for Se(IV): } \sigma = [SOH_2^+] - [SO^-] - [SSeO_3^-] \quad [20]$$

where σ is the surface charge (mol_c L^{-1}) related to surface potential by the following equation:

$$\sigma = \frac{CS_AC_p}{F}\psi \quad [21]$$

where C is the capacitance (F m^{-2}), S_A is the surface area (m^2 g^{-1}), and C_p is the solid suspension density (g L^{-1}).

The total numbers of reactive sites, SOH_T, are the adsorption maxima obtained by fitting the Langmuir isotherm equation to the adsorption data using the ISOTHERM nonlinear least squares optimization program (Kinniburgh, 1987) and are presented in Table 2. This calculation of adsorption maxima assumes that the adsorption isotherms conform to the Langmuir equation across the entire range of surface coverages, not just the limited range investigated in our study. The capacitance was

TABLE 2. Constant capacitance model parameters.

Soil	Total number of reactive sites, SOH_T†			
	Arsenite	Arsenate	Selenite	Selenate
	μmol kg^{-1}			
NE1 25–30	209.5	1084	357	462.5
NE1 35–40	337	3126	623.6	475.1
NE2 10–15	397.7	3402	652.9	1913
NE2 16–21	211.7	2324	609.4	243.6
NE3 50–54	390.9	5539	640.1	352.2
NE4 46–50	369	3266	728	641.4
SE1 48.5	161.1	2361	655.9	483.8
SE1 60	248.7	2569	548.4	494.1
SE2 23.5	93.59	771	411.4	1197
SE3 38.5	129.1	597.3	274	310.3
MW1 17	162	392	230.6	81.2
MW2 17	79.87	348.9	109.2	144.4
MW2 25	129.2	304.1	106	289.4
MW3 17	75.93	388.9	181.6	88.33
MW3 23	77.59	275.5	142.9	81.43

† Maximum adsorption obtained by nonlinear fitting of the Langmuir equation to the isotherm data using ISOTHERM (Kinniburgh, 1987).

fixed at C = 1.06 F m^{-2} as in previous constant capacitance modeling of Se(IV) (Goldberg and Glaubig, 1988a; Goldberg et al., 2007) and As(V) (Goldberg and Glaubig, 1988b; Goldberg et al., 2005) adsorption by soils. The protonation–dissociation constants were fixed at: log K_+(int) = 7.35 and log K_-(int) = −8.95. These values were averages of a literature compilation for Al and Fe oxides obtained by Goldberg and Sposito (1984) and have been used in prior constant capacitance modeling of As(V) adsorption by soils (Goldberg et al., 2005). Goodness of model fit was evaluated using the overall variance, V in Y:

$$V_Y = \frac{\text{SOS}}{\text{df}} \qquad [22]$$

where SOS is the weighted sum of squares of the residuals and df is the degrees of freedom (Herbelin and Westall, 1996).

Results and Discussion

Anion adsorption as a function of solution anion concentration is presented in Fig. 1 to 3. To avoid bias, we chose to show the first soil from each geographic region: NE1 25–30 from the Northeast, SE1 48.5 from the Southeast, and MW1 17 from the Midwest. The adsorption isotherms for adsorption of As(V), As(III), and Se(IV) are Langmuirian in shape, in that adsorption tends toward a maximum for high solution anion concentration. In contrast, the adsorption isotherms for Se(VI) adsorption are almost linear, conforming to a distribution coefficient model.

The constant capacitance model was fit to the anion adsorption isotherms, optimizing one surface complexation constant for each anion: log $K^2_{\text{As(V)}}$(int) for As(V), log $K^1_{\text{As(III)}}$(int) for As(III), log $K^2_{\text{Se(VI)}}$(int) for Se(VI), and log $K^2_{\text{Se(IV)}}$(int) for Se(IV). Table 3 provides values of the optimized surface complexation constants for each anion, as well as goodness-of-fit parameters, V_Y, for each optimization. The fits represented in Fig. 1 to 3 indicate the ability of the constant capacitance model to describe As(III) (Fig. 1a, 2a, and 3a), As(V) (Fig. 1b, 2b, and 3b), Se(IV) (Fig. 1c, 2c, and 3c), and Se(VI) (Fig. 1d, 2d, and 3d) adsorption isotherms. Except for one data point for As(V) adsorption by the SE1 48.5 soil, the model provides an excellent quantitative description of the adsorption behavior of the four anions by soils from three geographic locations having diverse mineralogy. Adsorption data and model fits for the remaining soils are available on the U.S. Salinity Laboratory website (www.ars.usda.gov/Services/docs.htm?docid=8908; verified 26 Sept. 2008). Our study represents the first description of As(III), As(V), Se(IV), and Se(VI) adsorption by soils as a function of equilibrium solution As(III), As(V), Se(IV), and Se(VI) concentrations.

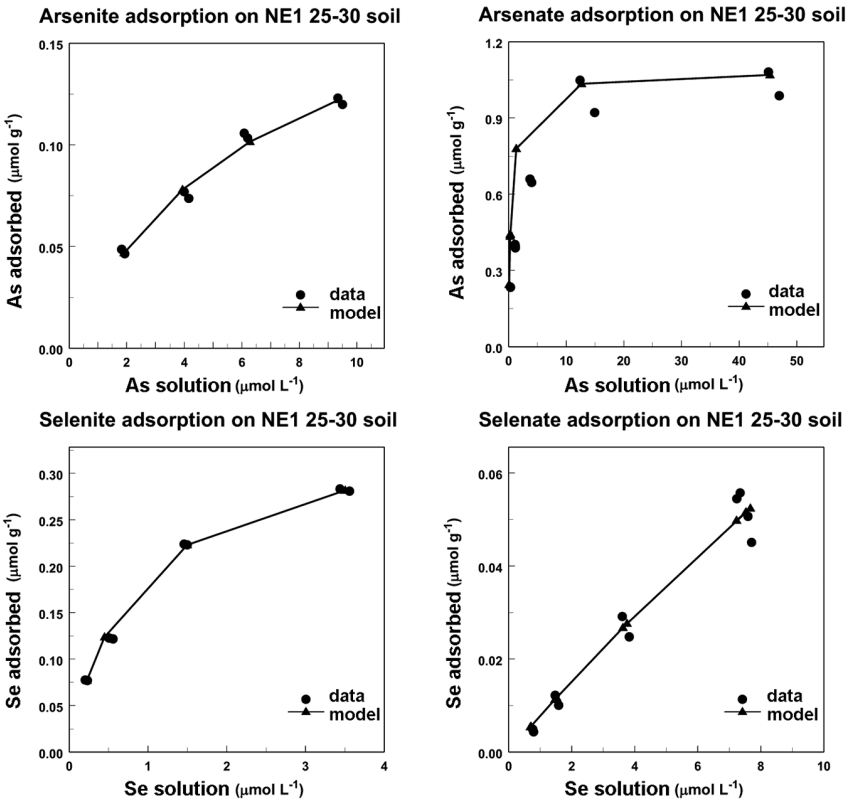

FIG. 1. Fit of the constant capacitance model to anion adsorption by the NE1 25–30 soil: (a) arsenite; (b) arsenate; (c) selenite; and (d) selenate. Circles represent experimental data. Model fits are represented by solid lines.

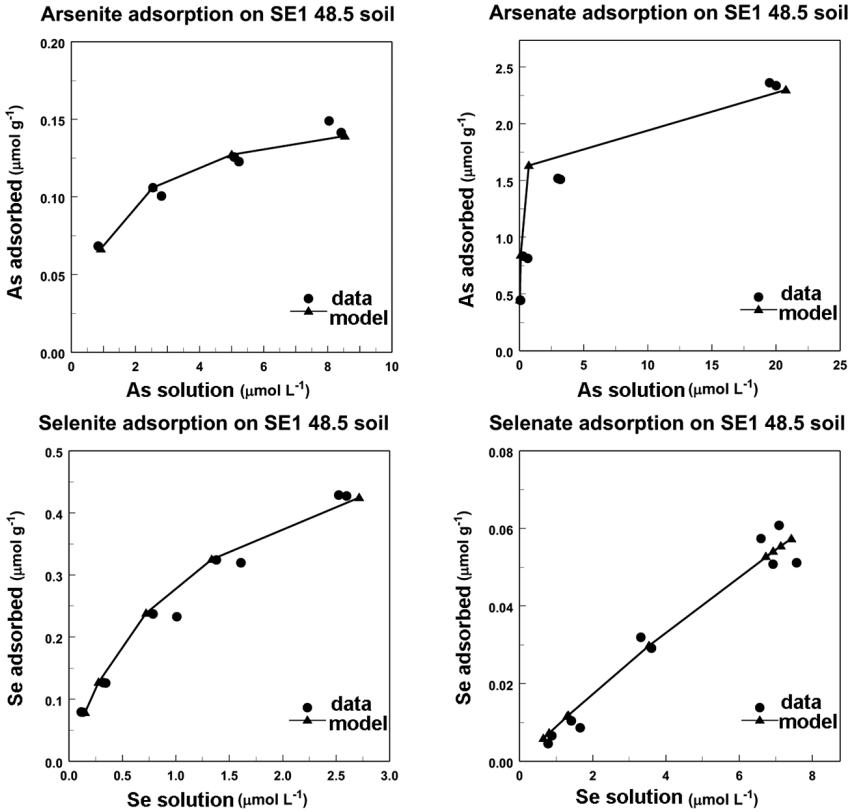

FIG. 2. Fit of the constant capacitance model to anion adsorption by the SE1 48.5 soil: (a) arsenite; (b) arsenate; (c) selenite; and (d) selenate. Circles represent experimental data. Model fits are represented by solid lines.

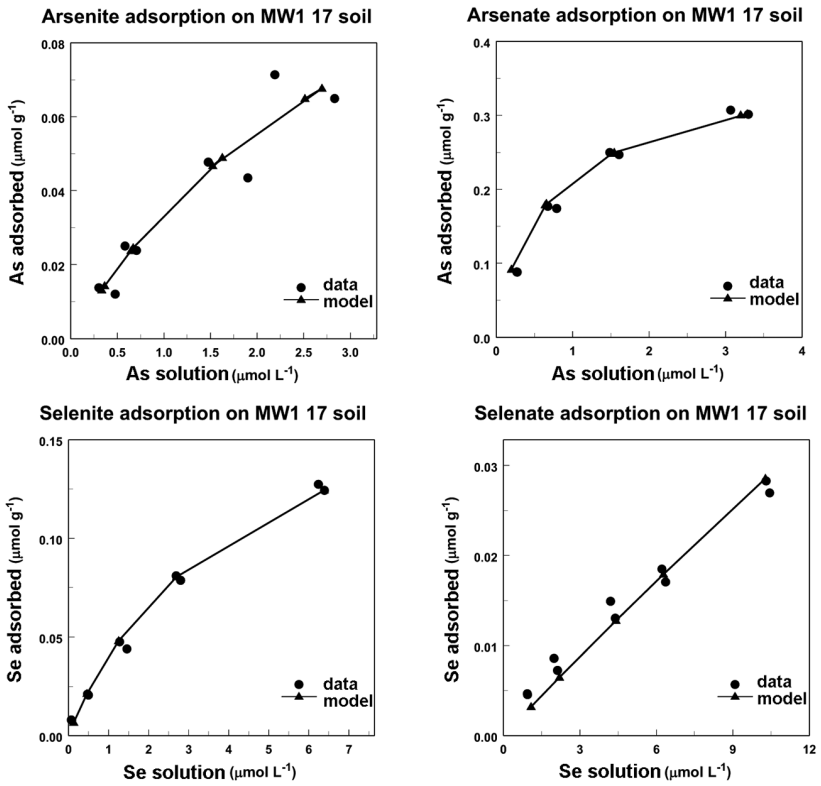

FIG. 3. Fit of the constant capacitance model to anion adsorption by the MW1 17 soil: (a) arsenite; (b) arsenate; (c) selenite; and (d) selenate. Circles represent experimental data. Model fits are represented by solid lines.

In prior work (Burns et al., 2006; Hyun et al., 2006), the coefficients that resulted from the generic Freundlich adsorption model fits were used to calculate distribution coefficients for As(III), As(V), Se(IV), and Se(VI) at a designated equilibrium solution concentration (~1.3 μmol L^{-1}). Simple and multiple linear regression analyses were conducted using these simplified coefficients to correlate anion adsorption and various soil properties (Burns et al., 2006; Hyun et al., 2006). Based on the regression coefficient values (R^2) for single and paired parameter correlations, correlations for As(V) and Se(IV) were highest (R^2 = 0.851 and 0.884, respectively, both significant at $P < 0.001$) when coupling average isotherm pH with 15-s DCB-extractable Fe, considered to represent the most available and reactive portion of the Fe oxides. The same correlation was also high for Se(VI) (R^2 = 0.818, $P < 0.001$), but pH coupled to clay produced a slightly higher correlation (R^2 = 0.836, $P < 0.001$). For As(III), pH coupled to oxalate-extractable Fe resulted in the best correlation (R^2 = 0.725, $P < 0.001$). Good correlations occurred for all species when pH was coupled to DCB-extractable Al as well (R^2 from 0.573, $P < 0.05$, to 0.794, $P < 0.001$). A similar multiregression analysis was performed with the constant capacitance model surface complexation constants for these anions. A subset of paired parameter regressions, including those that exhibited the highest correlations, are shown in Table 4. High correlations were again noted for coupled pH and Fe oxide, Al oxide, and clay content parameters as shown in Fig. 4, in agreement with the prior studies (Burns et al., 2006; Hyun et al., 2006). Overall, these results are consistent with other literature observations regarding pH dependence and the dominant role that Fe and Al oxides play in adsorption of As(V) and Se(IV) by soils (e.g., Goldberg et al., 2005, 2007).

The constant capacitance model was able to describe, for the first time, As(III), As(V), Se(IV), and Se(VI) adsorption on soils from these three utility sites as a function of solution anion concentration by optimizing only one surface complexation constant. Our study is the first application of the model to describe As(III) and Se(IV) adsorption by soils. The constant capacitance model explicitly includes the pH variable. Therefore, this chemical model constitutes an advancement over distribution coefficient and Langmuir and Freundlich isotherm models, which, despite containing two empirical adjustable parameters, cannot predict changes in adsorption occurring with changes in solution pH. Surface complexation constant values obtained in our study for the constant capacitance model can be incorporated into chemical speciation transport models to provide simulations and predictions of As and Se concentrations in soil solutions under diverse environmental conditions.

Under transport conditions, oxyanion diffusion into micropores and nanopores might become rate limiting and soil physical parameters such as porosity, structure, and texture may need to be considered, as they usually are in chemical speciation transport models. The solid/solution ratio is a factor that can influence the extent of ion adsorption (Di Toro et al., 1986). Anion adsorption as a function of equilibrium solution anion concentration on soil minerals was found to be

TABLE 3. Constant capacitance model surface complexation constants [K^1(int) and K^2(int)] and goodness of fits.

Soil	log $K^2_{As(V)}$(int)	V_Y†	log $K^1_{As(III)}$(int)	V_Y	log $K^2_{Se(IV)}$(int)	V_Y	log $K^2_{Se(VI)}$(int)	V_Y
NE1 25–30	5.547	0.01	6.538	104	4.989	0.002	3.624	0.05
NE1 35–40	6.891	0.005	3.668	0.009	6.559	0.04	4.849	0.01
NE2 10–15	7.308	0.005	8.217	0.02	8.610	0.01	4.097	0.02
NE2 16–21	6.941	0.01	8.406	0.40	7.187	0.11	4.980	0.03
NE3 50–54	6.148	0.004	8.087	0.56	7.903	0.006	5.165	0.02
NE4 46–50	6.859	0.001	8.056	0.006	5.957	0.001	4.080	0.08
SE1 48.5	6.124	0.05	7.533	0.67	5.077	0.01	3.932	0.06
SE1 60	6.052	0.005	7.418	0.54	4.985	0.006	3.761	0.02
SE2 23.5	4.793	0.02	7.211	0.69	4.729	0.008	2.719	0.04
SE3 38.5	4.741	0.01	7.234	0.44	4.786	0.06	3.417	0.02
MW1 17	5.292	0.02	5.576	0.005	3.869	0.007	1.754	0.02
MW2 17	4.776	0.01	5.516	0.01	3.743	0.04	2.560	0.01
MW2 25	5.281	0.01	5.729	0.05	3.937	0.03	2.668	0.01
MW3 17	5.641	0.002	5.676	0.05	3.564	0.06	3.038	0.02
MW3 23	5.571	0.02	5.752	0.06	3.377	0.10	2.768	0.007

† Goodness-of-fit equals the sum of squares divided by the degrees of freedom (Eq. [22]).

Table 4. Regression equation describing the correlation of the surface complexation constant log K(int) and pH with clay, surface area, and various oxide contents.

log $K^1_{As(III)}$(int)			log $K^2_{As(V)}$(int)		
Regression equation	r^2	P	Regression equation	r^2	P
−0.72 pH† + 0.03 Clay‡ + 10.7	0.794	***	−0.33 pH + 0.05 Clay + 7.32	0.524	*
−0.77 pH + 0.01 S_A§ + 11.1	0.760	***	−0.47 pH + 0.01 S_A + 8.46	0.323	NS
−0.64 pH + 0.05 DCB-Fe¶ + 10.0	0.880	***	−0.33 pH + 0.05 DCB-Fe + 7.29	0.491	*
−0.72 pH + 1.23 DCB-Al¶ + 10.3	0.929	***	−0.40 pH + 1.29 DCB-Al + 7.46	0.611	**
−0.82 pH + 0.04 Ox-Fe# + 11.5	0.758	***	−0.44 pH + 0.30 Ox-Fe + 8.08	0.530	*
−0.74 pH + 2.21 Ox-Al# + 10.3	0.827	***	−0.46 pH + 2.03 Ox-Al + 7.78	0.410	*
−0.66 pH + 0.84 15s-DCB-Fe†† + 10.3	0.877	***	−0.34 pH + 0.89 15s-Fe + 7.47	0.531	*
log $K^2_{Se(IV)}$(int)			log $K^2_{Se(VI)}$(int)		
Regression equation	r^2	P	Regression equation	r^2	P
−0.50 pH + 0.06 Clay + 5.86	0.823	***	−0.71 pH + 0.11 Clay + 8.27	0.807	***
−0.54 pH + 0.03 S_A + 6.20	0.686	***	−0.80 pH + 0.04 S_A + 9.14	0.586	**
−0.71 pH + 0.02 DCB-Fe + 7.44	0.639	***	−0.61 pH + 0.13 DCB-Fe + 7.54	0.839	***
−0.74 pH + 0.67 DCB-Al + 7.45	0.668	***	−0.95 pH + 2.42 DCB-Al + 9.39	0.790	***
−0.72 pH + 0.32 Ox-Fe + 7.35	0.788	***	−1.13 pH + 0.51 Ox-Fe + 11.2	0.686	***
−0.78 pH + 1.01 Ox-Al + 7.68	0.628	***	−1.04 pH + 4.55 Ox-Al + 9.56	0.642	**
−0.58 pH + 0.93 15s-DCB-Fe + 6.54	0.775	***	−0.72 pH + 2.19 15s-Fe + 8.51	0.858	***

* Significant at the 0.05 level; NS, not significant at the 0.05 level.
** Significant at the 0.01 level.
*** Significant at the 0.001 level.
† Average isotherm pH.
‡ Clay content (%).
§ Surface area ($m^2\ g^{-1}$).
¶ Dithionite–citrate–bicarbonate extractable Fe or Al ($g\ kg^{-1}$).
# Oxalate (pH 3) extractable Fe and Al ($g\ kg^{-1}$).
†† Quickly (15-s) dissolved Fe in DCB solution ($g\ kg^{-1}$).

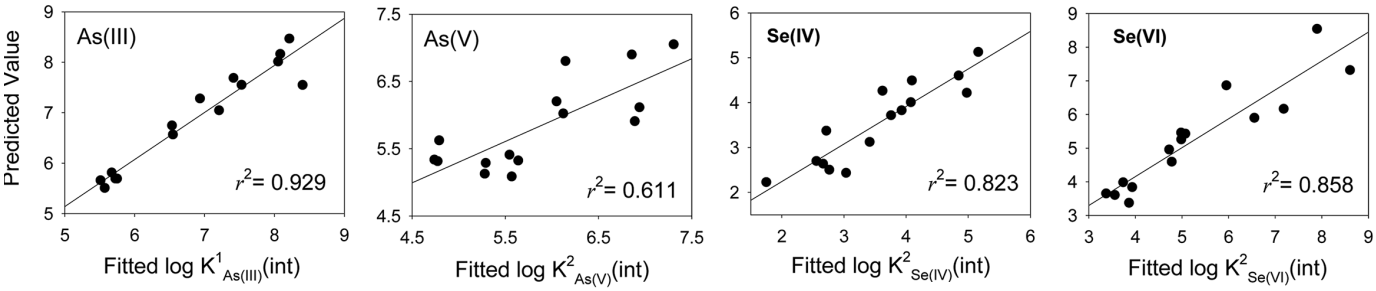

Fig. 4. Predicted value of surface complexation constants [K^1(int) and K^2(int)] obtained from regression equations that gives the highest r^2 values as detailed for each species: (a) log $K^1_{As(III)}$(int) = −0.72 pH + 1.23 DCB-Al + 10.3; (b) log $K^2_{As(V)}$(int) = −0.40 pH + 1.29 DCB-Al + 7.46; (c) log $K^2_{Se(IV)}$(int) = −0.50 pH + 0.06 Clay + 5.86; and (d) log $K^2_{Se(VI)}$(int) = −0.72 pH + 2.19 15sec-Fe + 8.51, where DCB-Al is dithionite–citrate–bicarbonate-extractable Al, and 15sec-Fe is quickly (15 s) dissolved Fe in DCB solution.

unaffected by changes in particle concentration over two orders of magnitude for molybdate adsorption by soil minerals (Goldberg and Forster, 1998). When particle concentration was increased by a factor of eight for adsorption of As on amorphous Al and Fe oxides, the ability of the constant capacitance model to describe the adsorption data was unaffected (Goldberg and Johnston, 2001).

Acknowledgments

Gratitude is expressed to Mr. H.S. Forster for technical assistance.

References

Adriano, D.C. 1986. Trace elements in the terrestrial environment. Springer, New York.

Agency for Toxic Substances and Disease Registry. 2000. Arsenic toxicity: Physiological effects. Available at www.atsdr.cdc.gov/csem/arsenic/physiologic_effects.html (verified 26 Sept. 2008). ATSDR, Atlanta, GA.

Agency for Toxic Substances and Disease Registry. 2003. Toxicological profile of selenium. Available at www.atsdr.cdc.gov/toxprofiles/tp92.pdf (verified 26 Sept. 2008). ATSDR, Atlanta, GA.

Balistrieri, L.S., and T.T. Chao. 1990. Adsorption of selenium by amorphous iron oxyhydroxide and manganese dioxide. Geochim. Cosmochim. Acta 54:739–751.

Bar-Yosef, B., and D. Meek. 1987. Selenium sorption by kaolinite and montmorillonite. Soil Sci. 144:11–19.

Burns, P.E., S. Hyun, L.S. Lee, and I. Murarka. 2006. Characterizing As(III, V) adsorption by soils surrounding ash disposal facilities. Chemosphere 63:1879–1891.

Catalano, J.G., Z. Zhang, P. Fenter, and M.J. Bedzyk. 2006. Inner-sphere adsorption geometry of Se(IV) at the hematite (100)–water interface. J. Colloid Interface Sci. 297:665–671.

Catalano, J.G., Z. Zhang, C. Park, P. Fenter, and M.J. Bedzyk. 2007. Bridging arsenate surface complexes on the hematite (012) surface. Geochim. Cosmochim. Acta 71:1883–1897.

Cihacek, L.J., and J.M. Bremner. 1979. A simplified ethylene glycol monoethyl ether procedure for assessing soil surface area. Soil Sci. Soc. Am. J. 43:821–822.

Cobo Fernandez, M.G., M.A. Palacios, and C. Camara. 1993. Flow-injection and continuous-flow systems for the determination of Se(IV) and Se(VI) by hydride generation atomic absorption spectrometry with on-line prereduction of Se(VI) to Se(IV). Anal. Chim. Acta 283:386–392.

Davis, J.A., J.A. Coston, D.B. Kent, and C.C. Fuller. 1998. Application of the surface complexation concept to complex mineral assemblages. Environ. Sci. Technol. 32:2820–2828.

de Brouwere, K., E. Smolders, and R. Merckx. 2004. Soil properties affecting solid–liquid distribution of As(V) in soils. Eur. J. Soil Sci. 55:165–173.

Del Debbio, J.A. 1991. Sorption of strontium, selenium, cadmium, and mercury in soil. Radiochim. Acta 52/53:181–186.

Di Toro, D.M., J.D. Mahony, P.R. Kirchgraber, A.L. O'Byrne, L.R. Pasquale, and D.C. Piccirilli. 1986. Effects of nonreversibility, particle concentration, and ionic strength on heavy metal sorption. Environ. Sci. Technol. 20:55–61.

Eary, L.E., D. Rai, S.V. Mattigod, and C.C. Ainsworth. 1990. Geochemical factors controlling the mobilization of inorganic constituents from fossil fuel combustion residues: II. Review of the minor elements. J. Environ. Qual. 19:202–214.

Elkhatib, E.A., O.L. Bennett, and R.J. Wright. 1984. Arsenite sorption and desorption in soils. Soil Sci. Soc. Am. J. 48:1025–1030.

Elsokkary, I.H. 1980. Selenium distribution, chemical fractionation and adsorption in some Egyptian alluvial and lacustrine soils. Z. Pflanzenernaehr. Bodenkd. 143:74–83.

Flower, B.A. 1977. Toxicology of environmental arsenic. p. 79–122. *In* R.A. Goyer and M.A. Mehlman (ed.) Toxicology of trace elements. John Wiley & Sons, New York.

Foster, A.L., G.E. Brown, and G.A. Parks. 2003. X-ray absorption fine structure study of As(V) and Se(IV) sorption complexes on hydrous Mn oxides. Geochim. Cosmochim. Acta 67:1937–1953.

Goldberg, S., and H.S. Forster. 1998. Factors affecting molybdenum adsorption by soils and soil minerals. Soil Sci. 163:109–114.

Goldberg, S., and R.A. Glaubig. 1988a. Anion sorption on a calcareous, montmorillonitic soil: Selenium. Soil Sci. Soc. Am. J. 52:954–958.

Goldberg, S., and R.A. Glaubig. 1988b. Anion sorption on a calcareous, montmorillonitic soil: Arsenic. Soil Sci. Soc. Am. J. 52:1297–1300.

Goldberg, S., and C.T. Johnston. 2001. Mechanisms of arsenic adsorption on amorphous oxides evaluated using macroscopic measurements, vibrational spectroscopy, and surface complexation modeling. J. Colloid Interface Sci. 234:204–216.

Goldberg, S., S.M. Lesch, and D.L. Suarez. 2007. Predicting selenite adsorption by soils using soil chemical parameters in the constant capacitance model. Geochim. Cosmochim. Acta 71:5750–5762.

Goldberg, S., S.M. Lesch, D.L. Suarez, and N.T. Basta. 2005. Predicting arsenate adsorption by soils using soil chemical parameters in the constant capacitance model. Soil Sci. Soc. Am. J. 69:1389–1398.

Goldberg, S., and G. Sposito. 1984. A chemical model of phosphate adsorption by soils: II. Noncalcareous soils. Soil Sci. Soc. Am. J. 48:779–783.

Gustafsson, J.P. 2001. Modelling competitive anion adsorption on oxide minerals and an allophane-containing soil. Eur. J. Soil Sci. 52:639–653.

Gustafsson, J.P. 2006. Arsenate adsorption to soils: Modelling the competition from humic substances. Geoderma 136:320–330.

Hall, M.L., and W.R. Livingston. 2002. Fly ash quality, past, present and future, and the effect of ash on the development of novel products. J. Chem. Technol. Biotechnol. 77:234–239.

Herbelin, A.L., and J.C. Westall. 1996. FITEQL: A computer program for determination of chemical equilibrium constants from experimental data. Rep. 96-01. Version 3.2. Dep. of Chemistry, Oregon State Univ., Corvallis.

Hyun, S., P.E. Burns, I. Murarka, and L.S. Lee. 2006. Selenium(IV) and (VI) sorption by soils surrounding fly ash management facilities. Vadose Zone J. 5:1110–1118.

Jackson, B.P., and W.P. Miller. 1998. Arsenic and selenium speciation in coal fly ash extracts by ion chromatography–inductively coupled plasma mass spectrometry. J. Anal. At. Spectrom. 13:1107–1112.

Jiang, W., S. Zhang, X. Shan, M. Feng, Y.-G. Zhu, and R.G. McLaren. 2005. Adsorption of arsenate on soils. Part 1. Laboratory batch experiments using 16 Chinese soils with different physiochemical properties. Environ. Pollut. 138:278–284.

Kinniburgh, D.G. 1987. ISOTHERM: A computer program for analyzing adsorption data. Version 2.2. Br. Geol. Surv., Wallingford, UK.

Ladeira, A.C.Q., V.S.T. Ciminelli, H.A. Duarte, M.C.M. Alves, and A.Y. Ramos. 2001. Mechanism of anion retention from EXAFS and density functional calculations: Arsenic (V) adsorbed on gibbsite. Geochim. Cosmochim. Acta 65:1211–1217.

Lumsdon, D.G., J.C.L. Meeussen, E. Pateson, L.M. Garden, and P. Anderson. 2001. Use of solid phase characterisation and chemical modelling for assessing the behavior of arsenic in contaminated soils. Appl. Geochem. 16:571–581.

Manning, B.A., S.E. Fendorf, and S. Goldberg. 1998. Surface structures and stability of arsenic(III) on goethite: Spectroscopic evidence for inner-sphere complexes. Environ. Sci. Technol. 32:2383–2388.

Masscheleyn, P.H., R.D. Delaune, and W.H. Patrick. 1990. Transformations of selenium as affected by sediment oxidation–reduction potential and pH. Environ. Sci. Technol. 24:91–96.

Masscheleyn, P.H., R.D. Delaune, and W.H. Patrick. 1991. Effect of redox potential and pH on arsenic speciation and solubility in a contaminated soil. Environ. Sci. Technol. 25:1414–1419.

Neal, R.H., and G. Sposito. 1989. Selenate adsorption on alluvial soils. Soil Sci. Soc. Am. J. 53:70–74.

Ona-Nguema, G., G. Morin, F. Juillot, G. Calas, and G.E. Brown. 2005. EXAFS analysis of arsenite adsorption onto two-line ferrihydrite, hematite, goethite, and lepidocrocite. Environ. Sci. Technol. 39:9147–9155.

Peak, D. 2006. Adsorption mechanisms of selenium oxyanions at the aluminum oxide/water interface. J. Colloid Interface Sci. 303:337–345.

Raven, K.P., A. Jain, and R.H. Loeppert. 1998. Arsenite and arsenate adsorption on ferrihydrite: Kinetics, equilibrium, and adsorption envelopes. Environ. Sci. Technol. 32:344–349.

Singh, M., N. Singh, and P.S. Relan. 1981. Adsorption and desorption of selenite and selenate selenium on different soils. Soil Sci. 132:134–141.

Singh, T.S., and K.K. Pant. 2004. Equilibrium, kinetics and thermodynamic studies for adsorption of As(III) on activated alumina. Sep. Purif. Technol. 36:139–147.

Smith, E., R. Naidu, and A.M. Alston. 1999. Chemistry of arsenic in soils: I. Sorption of arsenate and arsenite by four Australian soils. J. Environ. Qual. 28:1719–1726.

Sposito, G. 1982. On the use of the Langmuir equation in the interpretation of "adsorption" phenomena: II. The "two-surface" Langmuir equation. Soil Sci. Soc. Am. J. 46:1147–1152.

Sposito, G. 1983. Foundations of surface complexation models of the oxide–aqueous solution interface. J. Colloid Interface Sci. 91:329–340.

Sposito, G. 1984. The surface chemistry of soils. Oxford Univ. Press, Oxford, UK.

Sposito, G., J.C.M. de Wit, and R.H. Neal. 1988. Selenite adsorption on alluvial soils: III. Chemical modeling. Soil Sci. Soc. Am. J. 52:947–950.

Stumm, W., R. Kummert, and L. Sigg. 1980. A ligand exchange model for the adsorption of inorganic and organic ligands at hydrous oxide interfaces. Croat. Chem. Acta 53:291–312.

Suarez, D.L., S. Goldberg, and C. Su. 1998. Evaluation of oxyanion adsorption mechanisms on oxides using FTIR spectroscopy and electrophoretic mobility. ACS Symp. Ser. 715:136–178.

Turner, R.R. 1981. Oxidation state of arsenic in coal ash leachate. Environ. Sci. Technol. 15:1062–1066.

Wang, X., and X. Liu. 2005. Sorption and desorption of radioselenium on calcareous soil and its solid components studied by batch and column experiments. Appl. Radiat. Isot. 62:1–9.

Waychunas, G.A., B.A. Rea, C.C. Fuller, and J.A. Davis. 1993. Surface chemistry of ferrihydrite. Part 1. EXAFS studies of the geometry of coprecipitated and adsorbed arsenate. Geochim. Cosmochim. Acta 57:2251–2269.